RESEARCH ARTICLE

Evaluation of Structural Preservation Conditions for Shale Gas in Relict Syncline: A Case Study of Devonian-Carboniferous Strata in the Guizhou-Guangxi Area

Lingying Huang[1,2], **Yifan Gu**[1,2,*] **and Yuqiang Jiang**[1,2]

[1] State Key Laboratory of Oil and Gas Reservoir Geology and Exploitation, Southwest Petroleum University, Chengdu 610500, China
[2] School of Geoscience and Technology, Southwest Petroleum University, Chengdu 610500, China

Abstract

This study investigates the key factors controlling marine shale gas preservation in Devonian–Carboniferous strata, focusing on four representative synclines in the Nanpanjiang Basin and the northern margin of the Guizhong Depression: Langdai, Xinzhai, West Yizhou, and North Yizhou. Through tectonic characterization and balanced cross-section restoration, we clarify the effects of structural style, tectonic deformation intensity, and fault properties on shale gas preservation. Wide-gentle bidirectional thrust synclines (Xinzhai and West Yizhou) offer the most favorable preservation conditions, followed by the wide-gentle unidirectional thrust syncline (Langdai); the wide-gentle nappe-type thrust monocline (North Yizhou) is least favorable. The Yanshanian Period dominates tectonic shortening in three synclines, while the Indosinian Period is primary for North Yizhou. The Langdai area exhibits lower tectonic shortening rates (13.24% and 12.49% for Langdai and Xinzhai, respectively) and thinner denudation (1500–1800 m) than the Guizhong area (2500–5000 m), both conducive to preservation. Compressional reverse faults predominate throughout, enhancing lateral sealing. Quantitative evaluation identifies Type I favorable zones within the Xinzhai and Langdai synclinal cores, whereas Middle Devonian strata in West Yizhou and North Yizhou are classified as Type III owing to fault disruption and denudation. These findings provide a theoretical basis for shale gas exploration in the structurally complex Yunnan–Guizhou–Guangxi region.

Keywords: shale gas preservation, syncline structural model, tectonic shortening rate, Nanpanjiang Basin; Guizhong depression.

Submitted: 02 May 2026
Accepted: 20 June 2026
Published: 09 July 2026

Vol. 2, **No.** 4, 2026.
10.62762/JGEE.2026.303617

***Corresponding author:**
✉ Yifan Gu
xnsygyf@126.com

Citation
Huang, L., Gu, Y., & Jiang, Y. (2026). Evaluation of Structural Preservation Conditions for Shale Gas in Relict Syncline: A Case Study of Devonian-Carboniferous Strata in the Guizhou-Guangxi Area. *Journal of Geo-Energy and Environment*, 2(4), 244–264.

1 Introduction

Shale gas, an unconventional natural gas resource characterized by widespread distribution, substantial development potential, and environmentally favorable low-carbon attributes, has emerged as a core strategic resource for ensuring China's energy security and advancing the green transformation of its energy infrastructure [1, 2]. Since 2024, China's annual shale gas production has stabilized above 25 billion cubic meters, signaling a robust trajectory toward large-scale commercial development. The shale formations enabling commercial shale gas extraction in China are primarily located in the Early Paleozoic Wufeng-Longmaxi formations within the Sichuan Basin and its surrounding areas, with proven reserves accounting for more than 80% of the national total. In contrast, shale gas exploration in other oil- and gas-bearing basins in southern China remains in its initial stages [3–5]. Previous investigations have documented hydrocarbon seeps, bitumen deposits, paleo-oil reservoirs, and other manifestations of hydrocarbon occurrence throughout the Hunan-Guangxi-Guizhou region. Analysis of drilling core samples further demonstrates that this area holds significant potential for hydrocarbon resource exploration. Devonian to Carboniferous marine shales are extensively developed in the Yunnan-Guizhou-Guangxi region, characterized by wide distribution, substantial single-layer thickness, high total organic carbon (TOC) content, and an appropriate level of thermal maturity. Specifically, the shale thickness in the Guizhong Depression ranges from 470 to 1,300 meters, the total organic carbon (TOC) content varies between 0.5% and 10%, and the average vitrinite reflectance (Ro) generally exceeds 1.8%, indicating an overall dry gas generation stage. This provides a favorable material foundation for the generation and accumulation of shale gas [3, 6, 7].

In recent years, advancements in technologies such as refined 3D seismic data acquisition, processing, and interpretation, combined with in-depth research on shale reservoir geology and gas-bearing properties [6, 8] and the establishment of the core theoretical framework of "rift trough sedimentation controlling reservoir, deep-water facies controlling hydrocarbon generation, and secondary rift trough tectonic preservation" [7], have led to significant breakthroughs in shale gas exploration in the Nanpanjiang Basin and Guizhong Depression. However, large-scale exploration breakthroughs in this region remain elusive, constrained by complex geological conditions—including multiphase tectonic evolution and protracted episodes of uplift and erosion [9]—coupled with a relatively nascent exploration history [3, 6, 10].

This paper systematically analyzes the impacts of syncline tectonic characteristics and tectonic evolution on shale gas preservation in the Langdai, Xinzhai, West Yizhou, and North Yizhou synclines within the Yunnan-Guizhou-Guangxi region. Key factors such as structural models, the intensity of tectonic evolution, and fault properties are examined using methods including high-resolution seismic data interpretation and balanced cross-section restoration. Combined with quantitative evaluation methods, this study reveals the controlling mechanisms of shale gas preservation under complex tectonic settings, identifies favorable shale gas preservation units, and thereby provides theoretical support and technical guidance for shale gas exploration and development in the complex tectonic regions of Yunnan, Guizhou, and Guangxi.

2 Geological Setting

The Nanpanjiang Basin and the northern margin of the Guizhong Depression are situated at the tectonic junction between the southern margin of the Yangtze Block and the South China Caledonian Fold Belt. This area lies within a complex overlapping zone of the Tethys and the circum-Pacific major tectonic domains, with its structural framework closely linked to the tectonic evolution of the Youjiang Basin [11–15]. This area is bounded to the west by the Northeastern Yunnan Thrust-Fold Belt; to the southwest by the Ailao Mountain Fold Belt; to the north by the Southern Guizhou Depression, Central Guizhou Uplift, and Wuling Fold Belt; to the northeast by the Xuefeng Mountain Uplift; to the east by the Guilin Depression and Dayao Mountain Uplift; and to the south by the West Damingshan Uplift, Maguan Uplift, and Shiwandashan Basin (Figure 1(a)). From the Devonian period onward, the study area transitioned into a rift basin stage under the influence of pervasive extensional tectonics, establishing an ancient geomorphological framework characterized by alternating platform and basin environments [7]. During the Devonian-Carboniferous period, rifted ocean basins were well developed, largely inheriting the pre-existing paleogeomorphic framework. From the Late Permian to the Middle Triassic, the area gradually transitioned into the foreland basin evolutionary stage, marking the end of marine

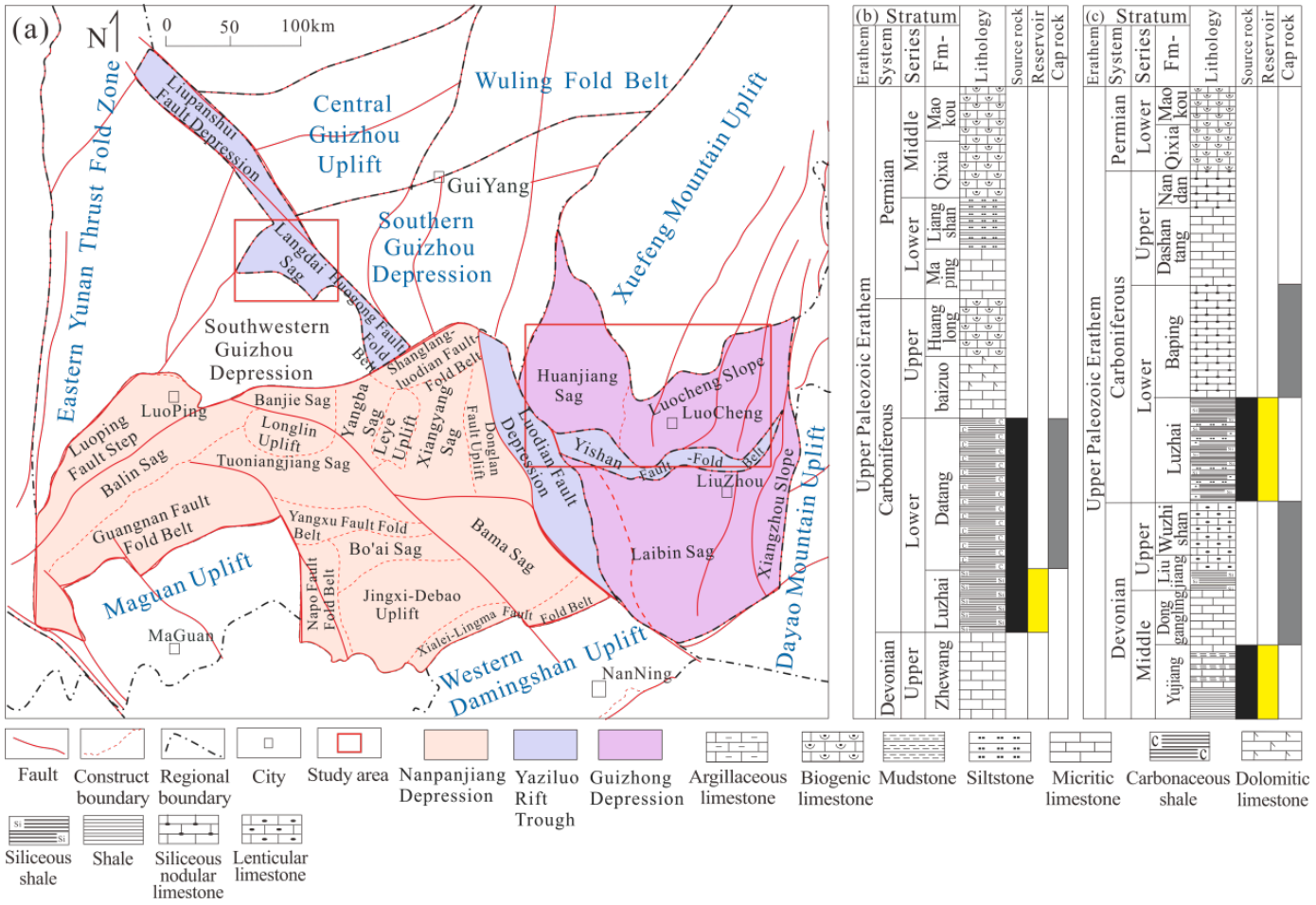

Figure 1. Geological Background of the Guizhou-Guangxi area. (a) Tectonic Location of the Nanpanjiang Depression and the Northern Margin of the Guizhong Depression. (b) Schematic Stratigraphic Columns of the Upper Paleozoic in Different Sedimentary Zones of the Nanpanjiang Basin. (c) Schematic Stratigraphic Columns of Different Sedimentary Zones in Northern Margin of the Guizhong Depression.

sedimentation.

Since the Late Jurassic, the study area has undergone a phase of prototype basin transformation similar to that documented in adjacent regions of southern China [16], experiencing intense uplift and erosion due to the Yanshan and Himalayan orogenies [2, 11, 17].

Based on differences in sedimentary environments, two stratigraphic division schemes have been established for the Upper Paleozoic strata in the Nanpanjiang area (Figure 1(c)), while three such schemes exist for the Upper Paleozoic strata in the Guizhong area (Figure 1(b)). The Nanpanjiang area is further subdivided into shallow-water and deep-water sedimentary zones, which display distinct lithological characteristics in the Upper Devonian to Upper Carboniferous strata. The northern margin of the Guizhong depression is divided into three major sedimentary zones: the continental sedimentary zone, characterized by vertical cyclic sedimentation of clastic and carbonate rocks; the platform-basin sedimentary zone, dominated by shale and limestone deposits; and the isolated platform sedimentary zone, consisting of multiple sedimentary cycles of light gray micritic limestone, grainy limestone, and bioclastic limestone. After the deposition of the Lower Permian, influenced by paleogeomorphic infilling and leveling processes, the lateral sedimentary differentiation among various sedimentary zones disappeared. Consequently, the lithologies within the Guizhong area and the Nanpanjiang area each tended to become homogeneous.

3 Analysis of Tectonic Characteristics and Evolutionary Processes

3.1 Fault Characteristics

The Langdai area adjoins the Yadu-Ziyun-Luodian Fault Zone, a regional deep-seated fault system predominantly comprising high-angle reverse faults

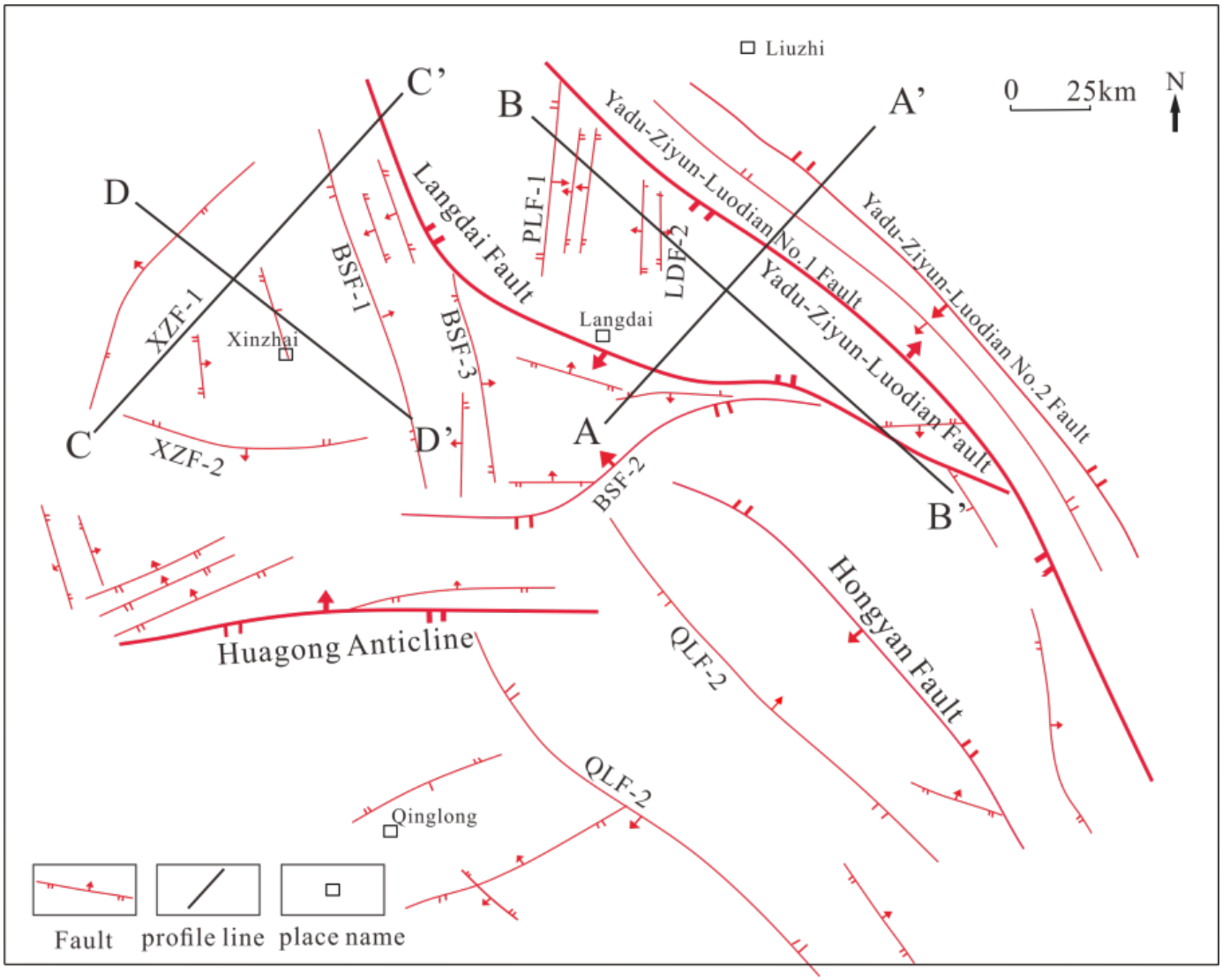

Figure 2. Fault distribution map of the Langdai area, Nanpanjiang Basin.

coupled with left-lateral strike-slip components [18, 19]. This fault zone has experienced multiple phases of tectonic activity and superimposed deformation, controlled by the superimposition of extensional forces following the closure of the Paleo-Tethys Ocean and intracontinental strike-slip extensional events during the Cenozoic Era, ultimately resulting in a complex tectonic framework [20]. Faults in the Langdai area are predominantly oriented northwest (NW), with locally developed northeast (NE)-trending faults (Figure 2). Based on a systematic analysis of fluid inclusions within the fractures of the fault zone, Xu et al. [2] proposed that these faults primarily formed during the Late Yanshanian–Himalayan period. This process may have altered shale gas preservation conditions, transitioning from early-stage sealed environments to late-stage open settings.

En echelon faults are extensively developed in the Guizhong area, where they are distributed in a zonal pattern and act as the controlling structures for the synclines within the study area (Figure 3), consistent with the regional fault framework documented in northern Guizhou [21].

The tectonic evolution of the North Yizhou Syncline area is governed by the Hechi-Yizhou-Liucheng Fault Zone, which contains the main controlling faults such as the Hechi-Yizhou Fault and the Yizhou Fault No. 1(YZF-1). This fault zone is accompanied by multiple nearly parallel secondary faults and, as a whole, exhibits transpressional tectonic characteristics, with the northern segment dominated by strike-slip and reverse movement. The overall strike of the fault zone is nearly east-west; however, local segments exhibit northwest (NW) or northeast (NE) orientations due to the superimposed effects of regional tectonics. The West Yizhou Syncline area is situated in the western

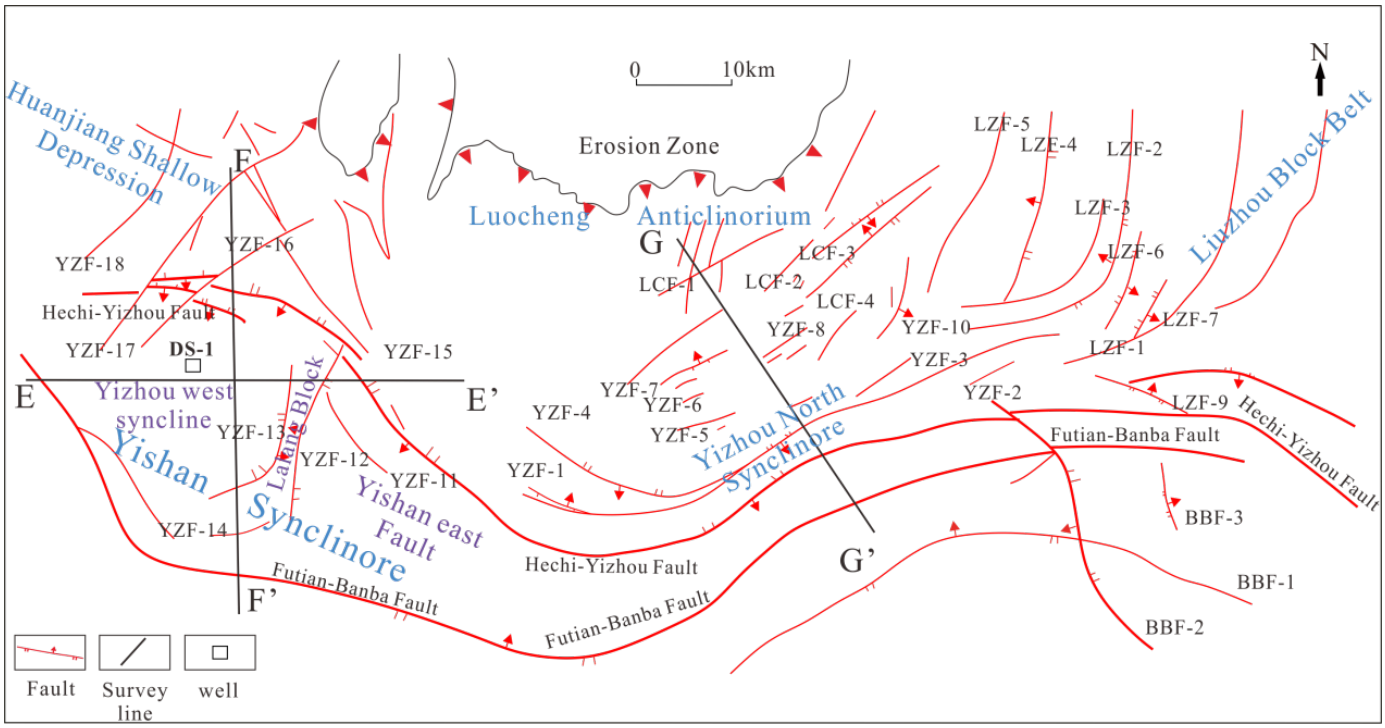

Figure 3. Fault distribution map of the northern margin of the Guizhong Depression.

segment of the Hechi-Yizhou-Liucheng Fault Zone. Faults in this region are predominantly strike-slip faults with minor reverse faulting characteristics. Major controlling faults, including the YZF-12, YZF-13, and YZF-17, are developed in the West Yizhou Syncline area. These faults are distributed in an "eyeball-shaped" pattern in plan view, with an overall strike of west-northwest. The main fault on the northern side dips toward the south-southwest, while the main fault on the southern side dips toward the north; the two main faults progressively converge toward the east and west. Near Hechi, the two main faults have undergone amalgamation, and the strike of the merged fault is approximately 310° (corresponding to northwest, NW) [22].

3.2 Typical Syncline Tectonic Units

3.2.1 Langdai Syncline

In plan view, the Langdai Syncline (Figure 4) displays a triangular configuration with a northwest-southeast orientation. Its northeastern end connects to the footwall of the Yadu-Ziyun-Luodian Fault on the southwest limb of the Hongyan Anticline. The southern side connects to the footwall of a reverse fault on the northern limb of the Bianshan Anticline, while the western side is cut by the Panlong Fault. The syncline covers a total area of approximately 335 km^2, with a major axis length of 31 km and a minor axis length of 14 km. The strata dip at angles ranging from 5° to 35°, exhibiting an overall broad configuration. The basement lithology of the Langdai Syncline is dominated by argillaceous limestone, interbedded with shale, siltstone, and carbonaceous shale, with localized occurrences of basalt, rendering the basement relatively rigid [20].

The deformation of the syncline is controlled by shear zones at its boundaries, exhibiting deformation characteristics of superimposed compression and shear; these features were identified through balanced cross-section restoration [23–25].

3.2.2 Xinzhai Syncline

The Xinzhai Syncline occupies the footwall of a reverse fault at the structural intersection between the northwestern limb of the NW-trending Bianshan Anticline and the northern limb of the NE-trending Huagong Anticline (Figure 4). It exhibits an overall wide-gentle structure. The western side of the syncline is controlled by the reverse fault and extends northeastward, with secondary faults developed at its base.

The syncline covers an area of approximately 190 km^2, with a major axis length of 17.0 km and a minor axis length of 14.5 km. The strata dip at angles ranging from 5° to 35°. The Xinzhai Syncline exhibits characteristics of multiple superimposed phases of deformation, and macroscopic fractures and interlayer cracks have developed within the syncline, analogous

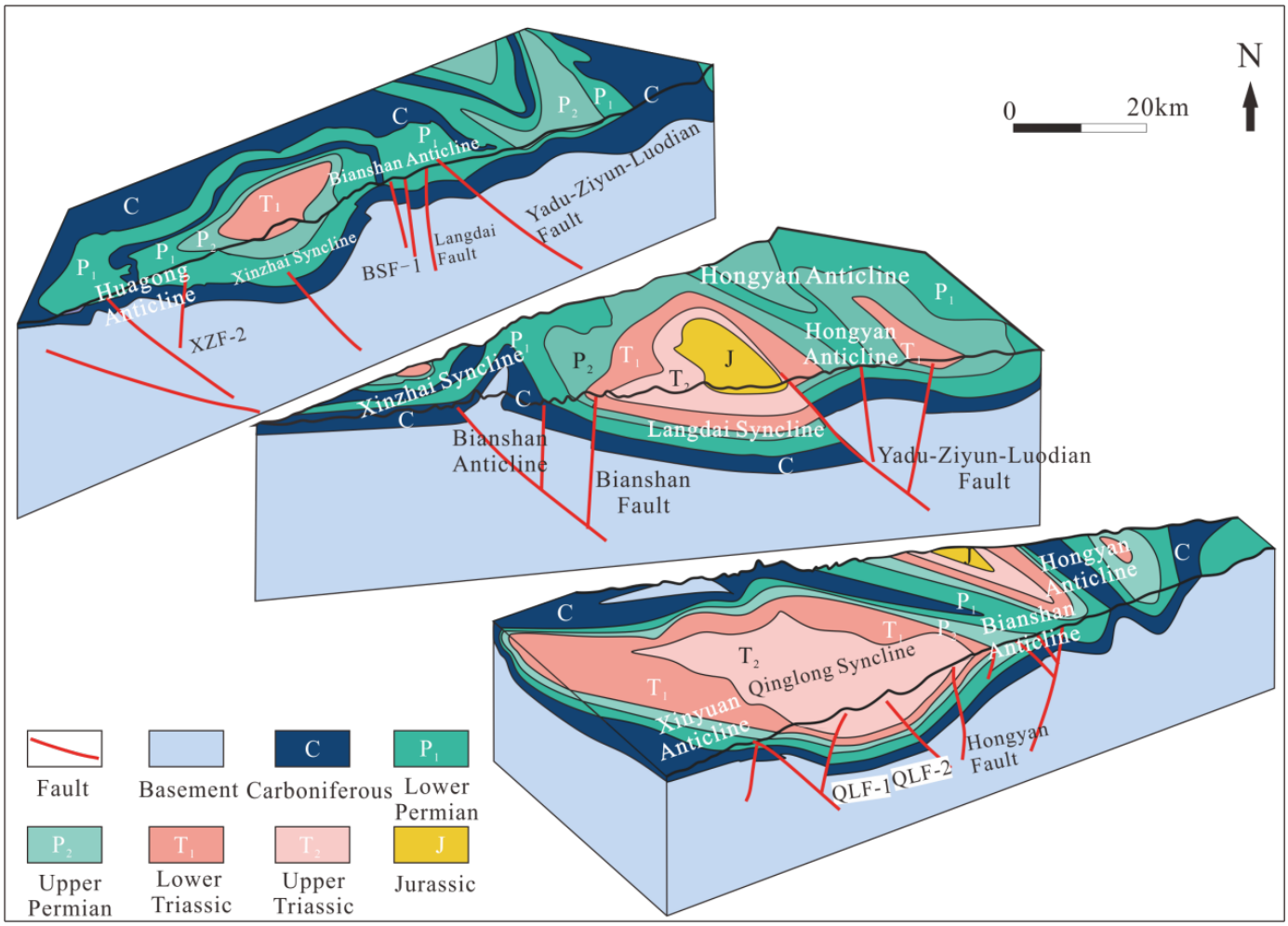

Figure 4. Tectonic sketch map of the Langdai area, Nanpanjiang Basin.

to deformation patterns observed in other synclines of the region [26].

3.2.3 *North Yizhou Syncline*

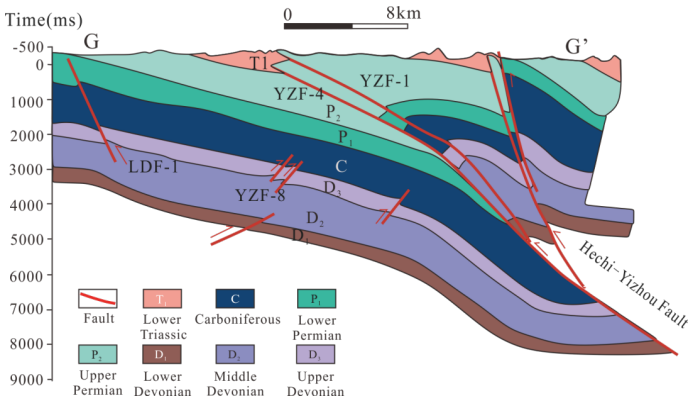

Figure 5. Tectonic sketch map of the Yizhou North syncline.

The North Yizhou Syncline (Figures 3 and 5) is situated on the northern limb of the Hechi-Yizhou Fault Zone and borders the Luocheng Compound Anticline to the north. Faults are well developed at the eastern end of the syncline, which exhibits a monocline structure that rises from south to north along the north-south axis. Faults are relatively underdeveloped on the northern limb, whereas the southern limb is truncated and overthrust by reverse faults. Covering a total area of 730 km^2, the syncline has a major axis length of 50 km and a minor axis length of 14 km, with strata dipping at angles ranging from 5° to 45°. The basement of the syncline consists of Neoproterozoic low-grade metamorphic gneiss and granulite. Its tectonic deformation was primarily influenced by Caledonian thrust-nappe movements, characterized by south-to-north nappe compression, with deformation intensity progressively decreasing toward the north [27].

3.2.4 *West Yizhou Syncline*

Controlled by the Futian-Banba Fault and the Hechi-Yizhou Fault, the Yishan Compound Syncline is segmented by the Lalong Fault Sag into three parts: the West Yizhou Syncline, the Lalong Fault Block, and the East Yishan Fault Block (Figure 3). The West Yizhou Syncline (Figure 6) is situated on the

western side of the Lalong Fault Block. Covering an area of approximately 460 km^2, the syncline has a major axis length of 30 km and a minor axis length of 22.1 km, with strata dipping between 2° and 10°. The formation of the syncline is closely associated with the left-lateral strike-slip movement of the Hechi-Yizhou Fault and the activity of north-south trending accommodation normal faults. Bounded and truncated by faults on all sides, the syncline exhibits an overall wide-gentle structure. It experienced minor reworking during late-stage compressional tectonism, resulting in limited fault development.

3.3 Tectonic Evolution Analysis Based on Balanced Cross-Section Restoration

Tectonic evolution was investigated primarily through the construction of balanced cross-sections utilizing seismic profiles integrated with back-stripping inversion techniques. Considering the stress direction, structural strike, fault distribution patterns, and actual production requirements of the study area, four seismic profiles arranged in a "two-horizontal and two-vertical" layout were selected as the key research targets along the northern margin of the Nanpanjiang Basin (Figure 2). In the northern margin of the Guizhong Depression, two seismic profiles arranged in a "one-horizontal and one-vertical" layout were selected in the West Yizhou Syncline area, and one seismic profile was selected in the North Yizhou Syncline area for the study of tectonic evolution characteristics (Figure 3).

3.3.1 Langdai Syncline

The results of the balanced cross-section restoration for the Langdai Syncline (Figure 7) reveal the following evolutionary stages: During the Middle Hercynian period, extensional stresses triggered normal faulting along the BSF-7 and YZLF-1 (Yadu-Ziyun-Luodian Fault No. 1), while the YZLF-3 exhibited minimal activity. A certain degree of uplift-subsidence differentiation existed between the Langdai Syncline area and its adjacent regions (Figures 7(e, j)).

During the Late Hercynian period, the extensional stress regime persisted. The normal faulting activity along BSF-7 and YZLF-1 intensified further, while YZLF-3 remained weakly active. Depressional features were observed near the hanging walls of these normal faults (Figures 7(d, i)).

During the Early Indosinian period, the tectonic stress field shifted to a nearly north-south compression, accompanied by right-lateral strike-slip movement. The early-formed normal faults, BSF-7 (Bianshan Fault No. 7) and YZLF-1, experienced thrust inversion. The deformation intensity during this stage was relatively low, and YZLF-3 also exhibited weak thrusting characteristics. Overall, uplift and subsidence features remained indistinct at this time (Figures 7(c, h)).

During the Late Indosinian period, the compressional stress field inherited from the Early Indosinian continued to dominate. The pre-existing BSF-7 and YZLF-1 exhibited more pronounced thrusting characteristics; in particular, the displacement along BSF-7 began to increase. YZLF-1 and YZLF-3 showed weak thrusting features, and the overall uplift-subsidence pattern started to take shape (Figures 7(b, g)).

During the Yanshanian-Himalayan period, characterized by a tectonic regime dominated by nearly east-west compression and left-lateral strike-slip movement, the pre-existing BSF-7 and YZLF-1 underwent significant thrusting activity. The displacements of BSF-7, YZLF-1, and YZLF-3 increased and subsequently stabilized. As a result, the Langdai Syncline was formed and ultimately finalized, exhibiting an asymmetric geometry with a gentle

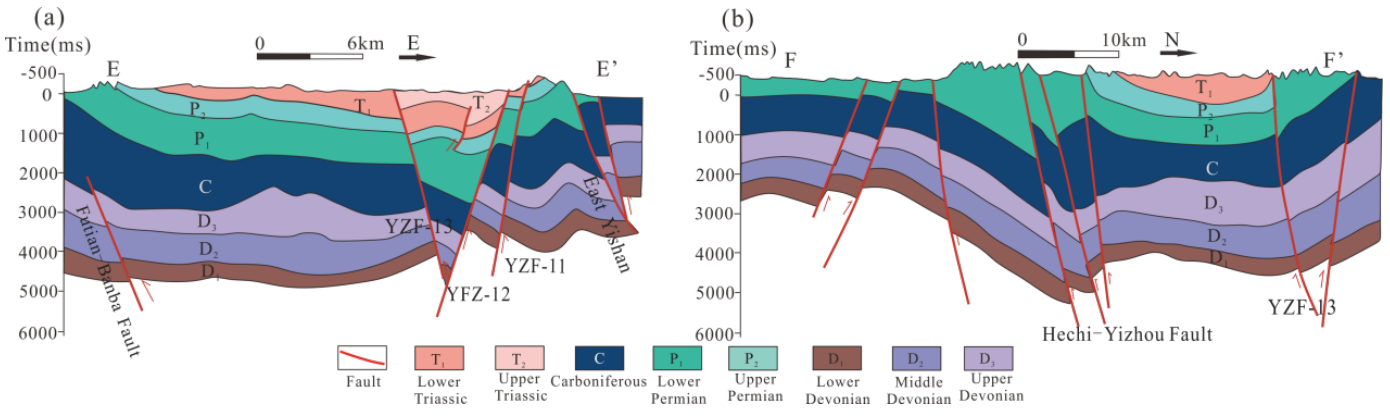

Figure 6. Tectonic sketch map of the Yizhou West syncline.

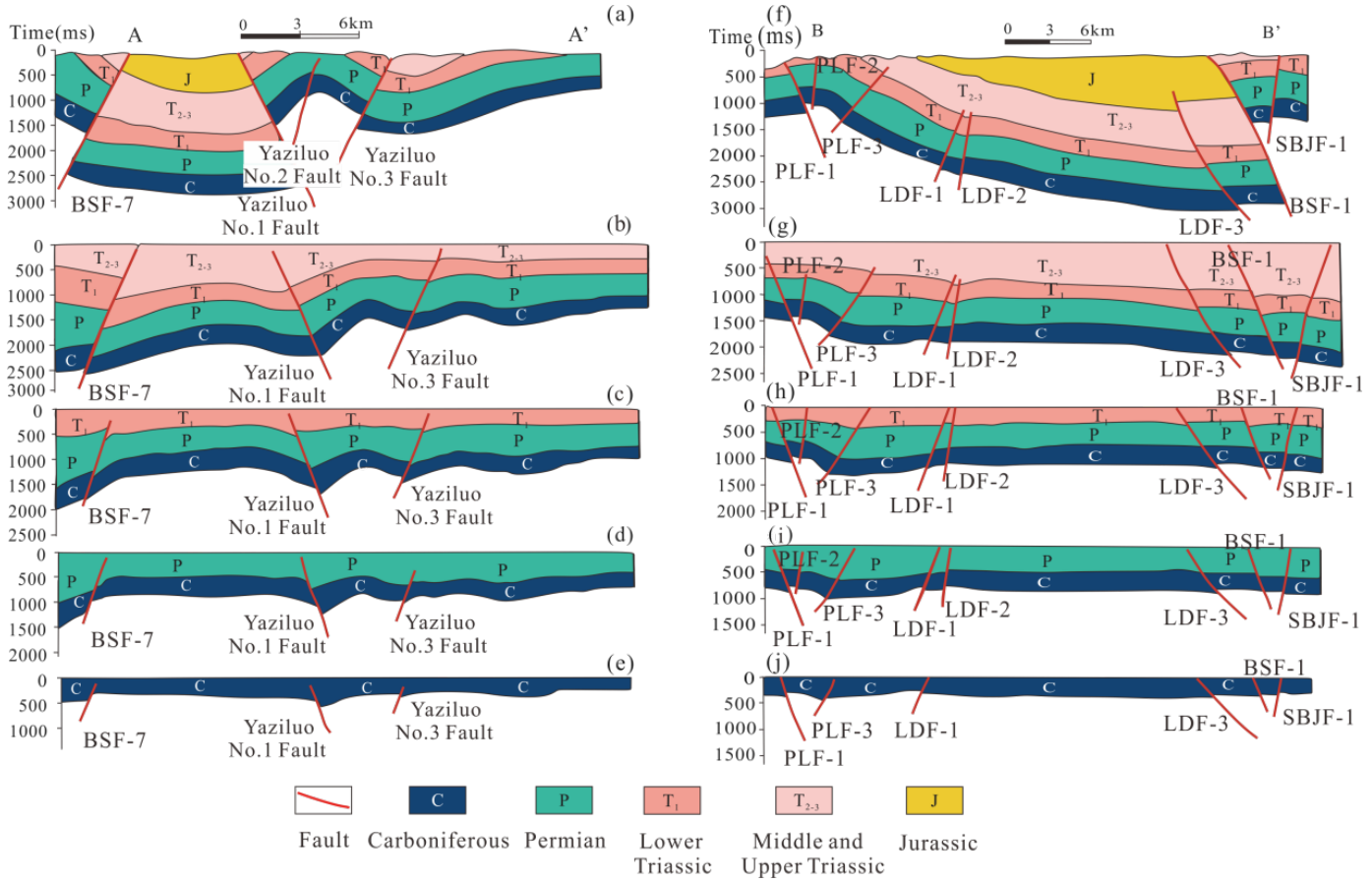

Figure 7. Cross-section restoration of the Langdai syncline. (a) Present-day section of Profile AA' ; (b) Section of Profile AA' before Jurassic deposition; (c) Section of Profile AA' before Middle–Late Triassic deposition; (d) Section of Profile AA' before Triassic deposition; (e) Section of Profile AA' before Permian deposition; (f) Present-day section of Profile BB' ; (g) Section of Profile BB' before Jurassic deposition; (h) Section of Profile BB' before Middle–Late Triassic deposition; (i) Section of Profile BB' before Triassic deposition; (j) Section of Profile BB' before Permian deposition.

northern limb and a steep southern limb (Figures 7(a, f)).

The primary deformation of the syncline occurred during the Yanshanian period, characterized by a relatively high tectonic shortening rate, defined as the percentage of contraction relative to the original length of strata after tectonic deformation [28]: 10.5% for Profile AA' and 7.9% for Profile BB' . The syncline preserves strata from the Jurassic to the Carboniferous systems relatively intact. Fault development follows an evolutionary pattern dominated initially by normal faults, followed by later thrust reversals and sustained intense activity.

3.3.2 *Xinzhai Syncline*

The results of the balanced cross-section restoration for the Xinzhai Syncline (Figure 8) reveal the following evolutionary stages: During the Middle Hercynian period, extensional stresses successively activated faults including XZF-1 (Xinzhai Fault No. 1), XZF-2, XZF-3, and BSF-7 (Figures 8(c, f)).

The Late Hercynian period sustained the extensional stress regime established during the Middle Hercynian. In this region, the activity of XZF-2 and XZF-3, as well as BSF-7, gradually intensified, while BSF-8 exhibited distinct normal faulting characteristics. During this time, the uplift and subsidence features had become relatively pronounced (Figures 8(b, e)).

During the Indosinian period, the strata experienced severe denudation, which made the restoration of the syncline structure quite challenging. Subjected to Indosinian compression, the characteristics of the early-formed faults underwent inversion, suggesting that the tectonic deformation was relatively intense.

During the Yanshanian-Himalayan period, under a tectonic stress regime dominated by nearly east-west compression, the activity of the XZF-2 and BSF-7 further intensified. In contrast, the activity of the XZF-3 diminished following the deposition of the Lower Permian, leading to the subsequent formation of the Xinzhai Syncline (Figures 8(a, d)).

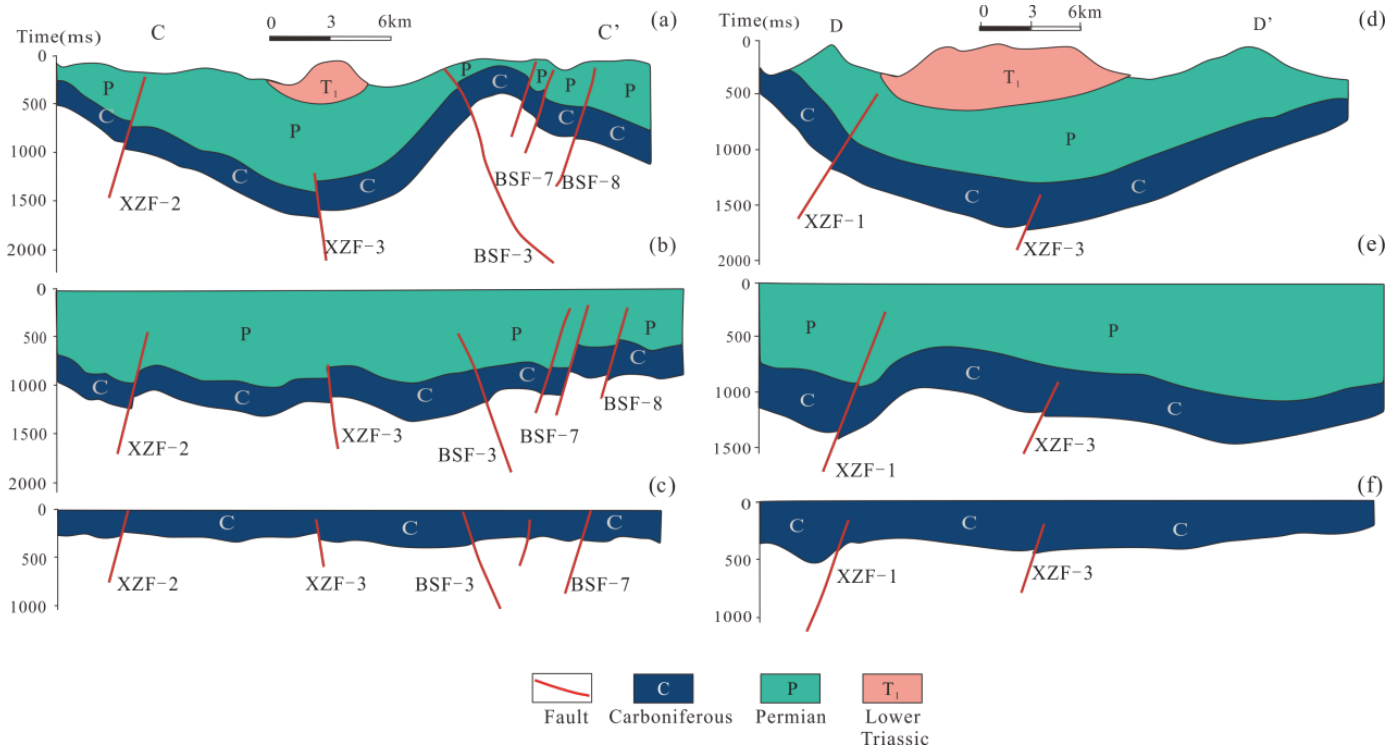

Figure 8. Cross-section restoration of the Xinzhai syncline. (a) Present-day section of Profile CC';(b) Section of Profile CC' before Triassic deposition;(c) Section of Profile CC' before Permian deposition;(d) Present-day section of Profile DD';(e) Section of Profile DD' before Triassic deposition;(f) Section of Profile DD' before Permian deposition.

The primary deformation of the syncline strata occurred during the Yanshanian period, characterized by relatively low tectonic shortening rates: 2.1% for Profile CC' and 1.6% for Profile DD' . The deformation intensity was weaker than that observed in the Langdai Syncline. Additionally, Jurassic and Middle to Late Triassic strata are absent within the syncline. Some faults ceased activity at an early stage, and the intensity of their late-stage thrusting was relatively low.

3.3.3 North Yizhou Syncline

The results of the balanced cross-section restoration for the North Yizhou Syncline (Figure 9) reveal the following evolutionary stages: Under regional extensional stresses during the Hercynian period, the Hechi-Yizhou Fault became active(Figure 9(d)).

During the Indosinian period, influenced by southeastward lateral compression and thrusting, the strata began to fold, forming a small anticline with new small faults such as LCF-1 (Luocheng Fault No. 1) and YZF-8. Meanwhile the activity of the YZF-4 and YZF-1 intensified (Figure 9(c)). During the Early Yanshanian period, the Jurassic and Cretaceous strata were completely denuded, making structural restoration particularly challenging. According to the research findings of Wu et al. [25] and Hu et al. [29], the study area was compressed by the northwest-southeast strike during the Early Yanshanian period, and was compressed by the north-northeast to south-southwest strike during the late Yanshan period. In the meantime, the YZF-4 and YZF-1 experienced thrust-nappe movement, and the syncline was essentially finalized (Figure 9(b, a)). During the Late Himalayan period, the North Yizhou Syncline area was characterized by uplift and denudation. Due to multiple phases of tectonic activity superimposed over time, the tectonic evolution of the syncline is challenging to reconstruct comprehensively.

The North Yizhou Syncline underwent intense deformation, with the Indosinian period marking its primary phase of deformation. During this time, the Indosinian-stage tectonic shortening rate reached 16.65%, contributing to a total tectonic shortening rate of 41.98%. Faults within the syncline predominantly display pronounced thrust-nappe characteristics. The syncline is characterized by widespread faults and prominent thrust nappe structures, with its final formation completed during the late Yanshanian period. Jurassic and Middle to Late Triassic strata are absent within the syncline, whereas Permian and Carboniferous strata are relatively well preserved.

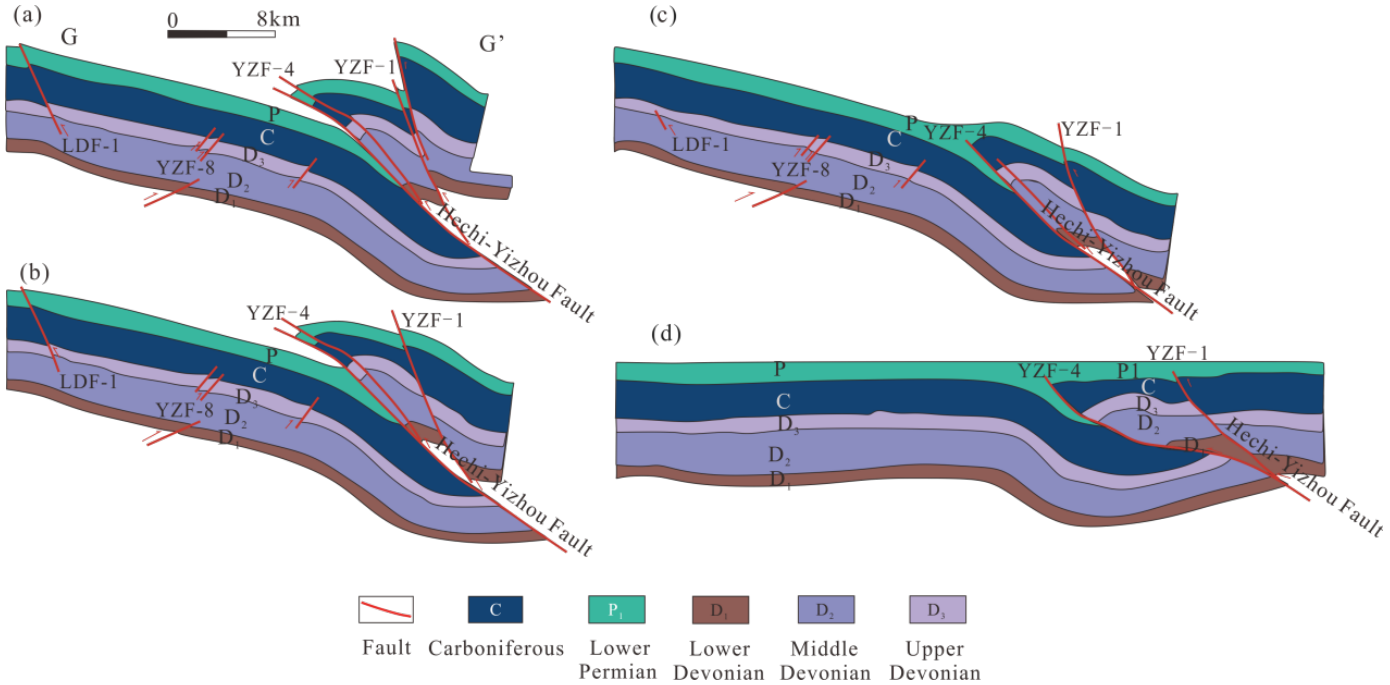

Figure 9. Cross-section restoration of the Yizhou North syncline. (a) Late Yanshanian section of Profile GG';(b) Early Yanshanian section of Profile GG';(c) Indosinian section of Profile GG';(d) Hercynian section of Profile GG'.

3.3.4 West Yizhou Syncline

The results of the balanced cross-section restoration for the West Yizhou Syncline (Figure 10) reveal the following evolutionary stages: Under the regional extensional stress regime during the Hercynian period, the major fault Futian-Banba Fault and East Yishan Fault became active, while minor faults Y13, Y12 and Y11 also showed slight activity(Figures 10(d, h)). During the Indosinian period, influenced by nearly north-south trending compressional folding, the early syn-sedimentary normal faults experienced tectonic inversion (Figures 10(c, g)). The Jurassic and Cretaceous strata in the profile were completely denuded, making it challenging to reconstruct the Early Yanshanian tectonic framework of this area. With reference to tectonic inversion characteristics documented in analogous basins [12], tectonic movement during the Early Yanshanian period is inferred to have been dominated by northwest-southeast trending compressional folding. Therefore, it is proposed that the YZF-13, YZF-12, and East Yishan Faults remained active, and the West Yizhou Syncline may have begun to form during this stage (Figures 10(b, f)).

In the late Yanshanian period, the main compressional folding occurred in the direction of north-northeast to south-southwest in the west Yizhou area, and the activity of Yizhou No.11, No.12 and East Yishan Fault intensified, and the thrusting of East Yishan Fault block likely occurred during this stage (Figures 10(a, e)).

Tectonic movement during the Early Himalayan period was dominated by nearly east-west trending compression, whereas it was characterized by regional uplift during the Late Himalayan period, which resulted in the complete denudation of strata. Combined with the superimposition of multiple phases of tectonic activity, the tectonic evolution of this area has become difficult to reconstruct comprehensively.

The core deformation stage of this syncline occurred during the Indosinian period, characterized by relatively high tectonic shortening rates: 7.3% for Profile EE' and 8.9% for Profile FF' . Jurassic and Middle to Late Triassic strata are absent within the syncline, whereas Permian and Carboniferous strata are relatively well preserved. All faults developed during the early stage exhibit normal faulting characteristics.

4 Main Controlling Factors for Shale Gas Preservation

4.1 Impacts of Tectonic factors for Shale Gas Preservation

4.1.1 Structural Models

Based on the integrated characteristics of reverse faults with varying orientations and associated folds, coupled with variations in structural forms (positive

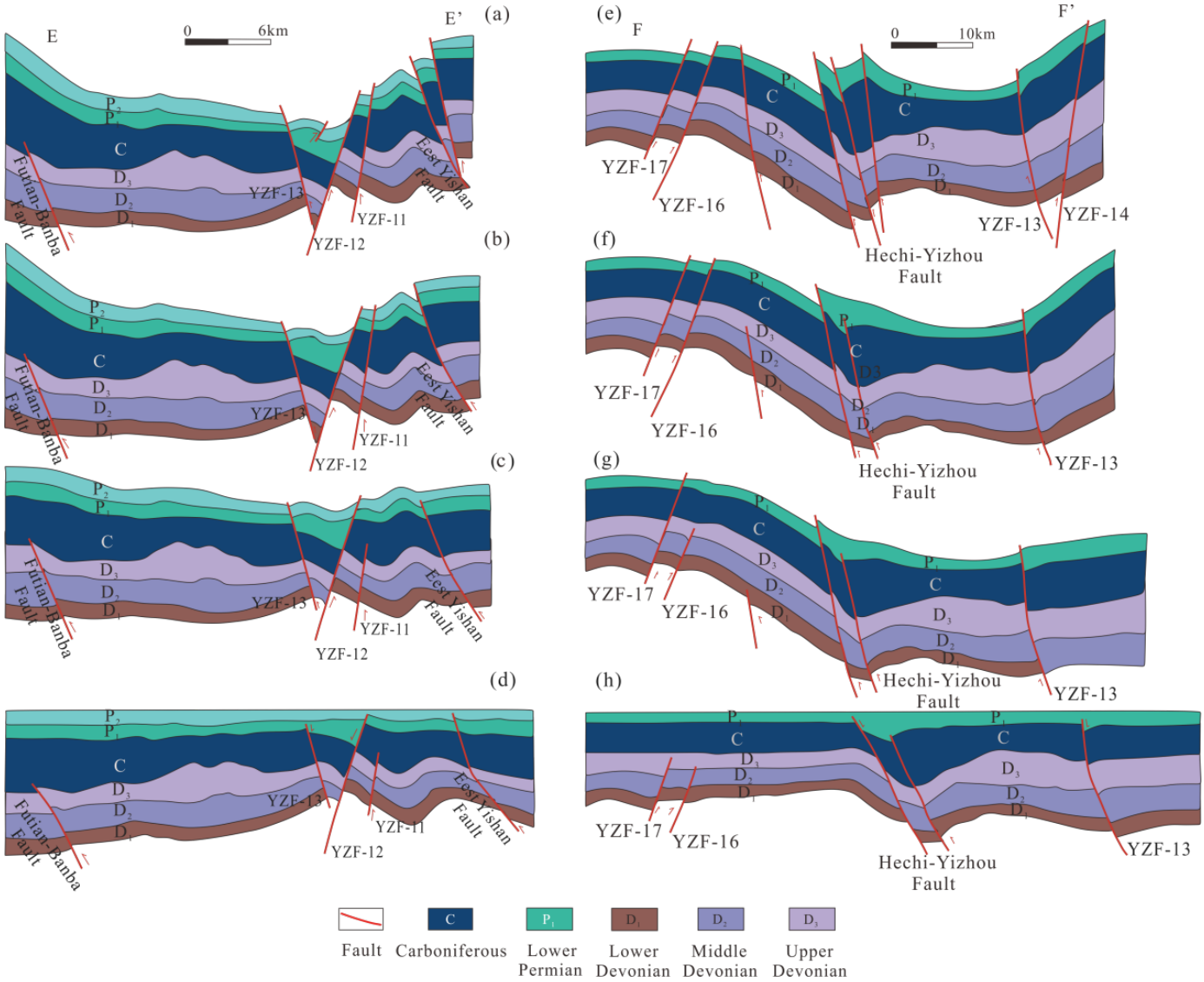

Figure 10. Cross-section restoration of the Yizhou West syncline.(a) Late Yanshanian section of Profile EE';(b) Early Yanshanian section of Profile EE';(c) Indosinian section of Profile EE';(d) Hercynian section of Profile EE';(e) Late Yanshanian section of Profile FF';(f) Early Yanshanian section of Profile FF';(g) Indosinian section of Profile FF';(h) Hercynian section of Profile FF'.

anticlinal,negative synclinal and oblique monocline) and structural tightness (wide-gentle, narrow-steep, and fractured), Jiang et al. [9] established 24 structural models for the differential enrichment of marine shale gas in South China (Figure 11). Building on this, further identification of synclines in the study area was conducted, and these synclines were classified into three synclinal structural models.

The Xinzhai Syncline and West Yizhou Syncline exhibit a structural model characterized by wide-gentle bidirectional thrust synclines. This model is also observed in the Changning Block and the Fuling Shale Gas Field in South China. Synclines of this type are distinguished by gently dipping limbs and an overall broad, gentle, and open structural configuration, primarily controlled by low-angle reverse faults [9, 30].

These synclines, extending from the limbs to the core, exhibit a gradual increase in burial depth, characterized by good stratigraphic continuity and relatively underdeveloped fault fractures. Moving from the shallow to the deeper parts of the syncline, the gas escape mechanism transitions from intense diffusion to weak diffusion, accompanied by an increase in pressure coefficient and an overall improvement in preservation conditions [28].

The Langdai Syncline exhibits a structural model characterized by a wide-gentle, unidirectional thrust syncline. In contrast to the wide-gentle, bidirectional thrust syncline, the core of the unidirectional thrust syncline features syncline-detached reverse faults,

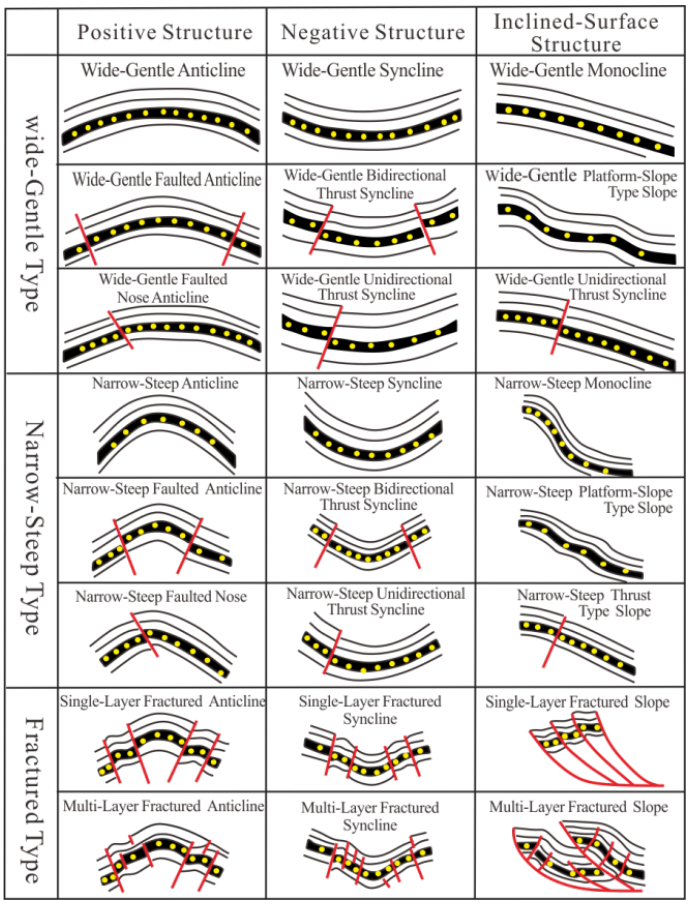

Figure 11. Structural model for differential enrichment of marine shale gas in South China [9].

where the fault displacement direction aligns with the fold's flexural-slip direction. These faults typically thrust the syncline structure in a single direction only. The shale gas preservation structural model for the wide-gentle, unidirectional thrust syncline depends on the gentle structural morphology, limited fault development, and favorable sealing conditions of both the upper and lower plates. When these conditions are met, this structural model reduces the risk of shale gas escape and promotes the formation of favorable shale gas reservoirs [28, 30].

The North Yizhou Syncline is characterized by a wide-gentle nappe-type thrust monocline structural model, which differs from the structural models previously classified by researchers based on cases in South China. Initially formed as an early syncline structure, this syncline was subsequently reworked by intense thrust-nappe movements, accompanied by the superimposed effects of uplift and denudation induced by thrust-nappe activity. Consequently, faults exhibit pronounced truncation effects on the strata, and the rocks are highly fragmented, resulting in poor shale gas preservation conditions. In the core of the North Yizhou Syncline, faults such as the LCF-8 and YZF-6 are relatively short and do not extend to the surface. Therefore, the deeply buried sections retain a certain capacity for shale gas preservation.

4.1.2 Tectonic Evolution

Tectonic evolution ultimately governs shale gas preservation by modulating the intensity of tectonic deformation, the degree of fault fragmentation, and the magnitude of uplift and denudation within synclines. In this study, the tectonic shortening rate was used as the primary index to quantify the intensity of tectonic evolution.

Elevated tectonic shortening rates indicate intensified regional compression, which consequently induces pronounced folding and faulting deformation in shale formations. This results in the development of densely distributed fault systems and fracture networks. Such intense tectonic reworking is often accompanied by an increase in both the number and connectivity of shale gas escape pathways, which is detrimental to shale gas preservation [32, 33]. Conversely, in areas characterized by low tectonic shortening rates and minimal tectonic deformation, fractures in shale formations remain relatively underdeveloped, with most fractures being semi-filled or unfilled. Low tectonic shortening rates result in a lack of escape pathways for late-stage natural gas, which promotes shale gas preservation in synclines [28].

Tectonic movements commonly trigger stratal uplift and denudation, which compromise caprock integrity, enhance fracture development, and diminish formation pressure, thereby profoundly affecting shale gas preservation. The later the timing of uplift and denudation, the smaller the denudation thickness, and the weaker the fault activity, the more favorable the conditions for shale gas preservation [9, 32, 33].

Statistics derived from the profile restoration results of synclines in the study area (Table 1) reveal the following: the North Yizhou Syncline exhibits the highest tectonic shortening rate (41.98%), while the Xinzhai Syncline has the lowest (12.49%). Additionally, the denudation thickness in the Langdai area is significantly less than that in the Guizhong area. Overall, the synclines in the study area are characterized by minor early-stage uplift, prolonged relative stability, and intense late-stage reworking.

The primary phases of uplift and denudation occurred during the Yanshanian and Himalayan periods, representing relatively late-stage denudation events.

The tectonic evolution characteristics of the four synclines indicate that the Langdai and Xinzhai Synclines offer the most favorable conditions for shale gas preservation, followed by the West Yizhou Syncline, while the North Yizhou Syncline exhibits the poorest shale gas preservation conditions.

4.1.3 Faults

Statistics on the fault characteristics of the Langdai area, conducted by Xu et al. [2] (Table 2), show that faults in this region are predominantly compressional reverse faults. Previous studies have indicated that fault movement in the Langdai area is characterized by thrust and left-lateral strike-slip motions [20]. A small number of normal faults, formed by late-stage tectonic inversion, are also present in the region. Additionally, some inverted faults have further subdivided the syncline into smaller fault blocks [35].

Notably, faults in the Langdai area generally extend to the shallow subsurface strata and intersect with one another, forming a complex fault network. However, the internal structure of the fault blocks is relatively simple, and the overall tectonic stability is good, providing favorable conditions for shale gas preservation [18, 25, 31].

Statistics on the fault characteristics of the northern margin of the Guizhong Depression (Table 3) indicate that faults in the Guizhong area are predominantly reverse faults. Although major faults such as the Futian-Banba Fault and the Hechi-Yizhou Fault exhibit significant throws (105–2800 m), they are

Table 1. Tectonic evolution characteristics of the four synclines in the study area.

Syncline Name	Initial Formation Period	Morphological Characteristics	Main Period of Strata Shortening	Total Tectonic Shortening Rate (%)	Denudation Thickness (m)
Langdai Syncline	Early Yanshanian	Narrow triangular shape, steep in the north and gentle in the south	Late Yanshanian (E–W); Early Yanshanian (N–S)	16.1% (E–W); 13.24% (N–S)	1500–1800 (According to Feng et al. [34])
Xinzhai Syncline	Indosinian	Symmetrical, gentle and sub-circular shape, steep in the east and gentle in the west	Late Yanshanian (E–W); Early Yanshanian (N–S)	16.4% (E–W); 12.49% (N–S)	—
West Yizhou Syncline	Early Yanshanian	Gentle sheet shape, steep in the west and gentle in the east, steep in the north and gentle in the south	Late Yanshanian (E–W); Early Yanshanian (N–S)	19.11% (E–W); 24.71% (N–S)	2500–5000 (According to Qin et al. [3])
North Yizhou Syncline	Indosinian	Narrow strip shape, steep in the north and gentle in the south	Early Yanshanian (N–S)	41.98% (N–S)	—

Table 2. Fault characteristics of the Langdai area, Nanpanjiang Basin [2].

No.	Fault Name	Fault Type	Fault Properties	Extension Length (km)	Throw (m)	Strike Direction	Dip Direction
1	YZLF	Reverse Fault	Positive Inversion	54.5	1365	NW	NE
2	YZLF-1	Reverse Fault	Compressional	36.3	292	NW	SW
3	YZLF-2	Reverse Fault	Positive Inversion	36.4	673	NW	SW
4	XZF-1	Reverse Fault	Compressional	16.5	223	NE	NW
5	XZF-2	Reverse Fault	Compressional	13.4	238	E–W	S
6	BSF-1	Reverse Fault	Compressional	21.5	269	NW	NE
7	BSF-2	Reverse Fault	Compressional	26.4	808	E–W	N
8	BSF-3	Reverse Fault	Compressional	13.2	356	NW	NE
9	LPS-LDF	Reverse Fault	Positive Inversion	47.8	1173	NW	SW
10	ZZF	Reverse Fault	Compressional	11.6	288	NW	E
11	HGF	Reverse Fault	Compressional	26.6	962	E–W	N
12	QLF-1	Reverse Fault	Compressional	36.6	481	NW	SW
13	QLF-2	Reverse Fault	Compressional	26.5	292	NW	NE
14	HYF	Reverse Fault	Compressional	28.7	827	NW	SW

Table 3. Fault characteristics of the northern margin of the Guizhong Depression.

No.	Fault Name	Fault Type	Extension Length (km)	Throw (m)	Strike Direction	Dip Direction
1	Futian Banba Fault	Reverse Fault	149.25	150–2100	E–W	N
2	Hechi-Yizhou Fault	Reverse Fault	160.46	150–2800	E–W	S
3	BBF-1	Reverse Fault	61.30	200–2190	E–W	N
4	BBF-2	Reverse Fault	33.09	170	NW	SW
5	BBF-3	Reverse Fault	7.55	190–500	NNW	E
6	LZF-1	Reverse Fault	36.46	120–300	NE	NW
7	LZF-2	Reverse Fault	34.63	120–530	NE	NW
8	LZF-3	Reverse Fault	21.80	110–650	NE	NW
9	LZF-4	Reverse Fault	21.47	120–300	NNE	NNW
10	LZF-5	Reverse Fault	20.97	90–200	NNE	NE
11	LZF-6	Reverse Fault	11.30	90–200	NNE	NE
12	LZF-7	Reverse Fault	7.34	90–150	NE	SE
13	LZF-8	Reverse Fault	25.85	190	E–W	S
14	LZF-9	Reverse Fault	11.40	360–1130	SE	NE
15	LCF-1	Reverse Fault	15.70	170–200	NE	SE
16	LCF-2	Normal Fault	11.24	50–150	NE	NW
17	LCF-3	Reverse Fault	13.17	70–150	NE	SE
18	LCF-4	Reverse Fault	17.97	70–150	NE	NW
19	YZF-1	Reverse Fault	61.86	200–2180	NEE	SSE
20	YZF-2	Reverse Fault	5.63	150–260	NE	SE
21	YZF-3	Reverse Fault	7.47	100–190	NE	SE
22	YZF-4	Reverse Fault	26.03	100–500	SE	S
23	YZF-5	Reverse Fault	6.55	100–300	NE	NW
24	YZF-6	Reverse Fault	8.17	60–220	NE	NW
25	YZF-7	Reverse Fault	17.19	110–170	NE	SE
26	YZF-8	Reverse Fault	6.02	60–100	NE	NW
27	YZF-9	Reverse Fault	6.92	100–210	NE	SE
28	YZF-10	Reverse Fault	9.69	60–140	NNE	SSE
29	YZF-11	Normal Fault	10.93	560–1130	NW	SW
30	YZF-12	Normal Fault	21.11	790–1600	NNE	NNW
31	YZF-13	Normal Fault	19.72	80–500	NNE	SEE
32	YZF-14	Reverse Fault	16.07	80–270	SE	NE
33	YZF-15	Normal Fault	29.70	80–310	NW	SW
34	YZF-16	Reverse Fault	23.27	220–1110	NE	SE
35	YZF-17	Normal Fault	32.62	80–380	NE	SE
36	YZF-18	Normal Fault	20.80	1000	NE	NW

transpressional reverse faults that can still provide favorable conditions for shale gas preservation.

A small number of normal faults with large throws, such as the LCF-1, have limited impact on preservation conditions due to their distance from the syncline core. Normal faults which develop around the margin of the West Yizhou Syncline, may adversely affect shale gas preservation in the marginal strata of the syncline.

4.2 Sealing Conditions

Sealing conditions for shale gas preservation refer to the capacity of caprocks to impede the upward migration of shale gas [34, 36]. Favorable sealing conditions effectively slow the escape of shale gas, maintain the pressure system within shale reservoirs, and protect these reservoirs from reworking and damage caused by late-stage fluids [34, 37]. In this study, the microscopic sealing capacity of shale gas caprocks was quantified by statistically analyzing the

Table 4. Microscopic sealing capacity of shale gas caprocks in the Langdai area and the northern margin of the Guizhong Depression.

No.	Area	Formation	Porosity (%)	Permeability (mD)	Breakthrough Pressure (MPa)
1	Langdai	Maokou	1.08	2.0×10^{-6}	25.6
2	Langdai	Qixia	1.84	5.0×10^{-6}	39.0
3	Langdai	Baizuo	2.75	3.3×10^{-5}	28.4
4	Langdai	Datang	2.06	5.2×10^{-5}	25.7
5	Guizhong	Simen	0.64	< 0.01	21.0
6	Guizhong	Baping	14.65	3.0×10^{-2}	0.9
7	Guizhong	Wuzhishan	1.39	< 0.01	22.5

Table 5. Evaluation index for shale gas preservation in the Nanpanjiang and northern margin of the Guizhong Depression.

Evaluation Parameter		Weight	Evaluation index		
			Type I	Type II	Type III
Burial Depth(m)		0.074	3000~4500	1500~2500	1500 or 4500
Stratum Dip Angle(°)		0.074	10	10~20	20
Cap Rock Conditions	Breakthrough Pressure	0.111	40MPa	20~40MPa	20MPa
	Roof Floor Lithology	0.074	Gypsum Rock, Mudstone	Dense Carbonate Rock	Siltstone
	Regional Cap Rock Distribution	0.074	Large-area Continuous	Relatively Large-area Continuous	Small-area Discontinuous Distribution
	Outcropping Strata	0.037	J,T	P	C
Tectonic	Structural model	0.111	wide-gentle bidirectional thrust synclines	wide-gentle, unidirectional thrust syncline	wide-gentle nappe-type thrust monocline
	Tectonic Shortening Rate	0.111	10~20	20~30	30
	Eroded Thickness	0.074	2000	2000~4000	4000
	Fault Property	0.111	Reverse Fault	Normal Fault	Strike-slip Fault
Distance to Target Bed Outcrop(km)		0.074	15	10~15	5~10
Distance to Deep-large Penetrating Faults (km)		0.074	5	3~5	1~3

porosity, permeability, and breakthrough pressure of caprocks or indirect caprocks in the Langdai area and the northern margin of the Guizhong Depression (Table 4).

In the Langdai area, Carboniferous strata are buried at depths ranging from 1,000 to 8,000 m, with well-developed regional caprocks characterizing the upper section. Specifically, both the top caprocks (Datang Formation and Baizuo Formation of the Carboniferous System) and the indirect caprocks (Upper Carboniferous to Lower Triassic Feixianguan Formation) exhibit low porosity and low permeability. The average porosity of the top caprocks is 1.94%, with an average permeability of 0.029×10^{-3} mD, while the indirect caprocks have an average porosity of 1.99% and an average permeability of 0.017×10^{-3} mD.

The overall breakthrough pressure of the caprocks ranges from 23.5 MPa to 61.6 MPa, with an average value of 35.1 MPa. This is significantly higher than the effective sealing threshold of 10.0 MPa, indicating an exceptionally strong sealing capacity of these caprocks [2].

At the northern margin of the Guizhong Depression, the burial depth of the Carboniferous basal boundary ranges from 800 to 3,800 m. The sealing performance of caprocks varies significantly among different strata. The limestone of the upper Baping Formation exhibits a porosity of up to 14.65% and a breakthrough pressure of only 0.9 MPa, indicating the poorest sealing capacity among the investigated formations. In contrast, the limestone of the Simen Formation is characterized by low porosity (1.99%) and low permeability (0.03 mD),

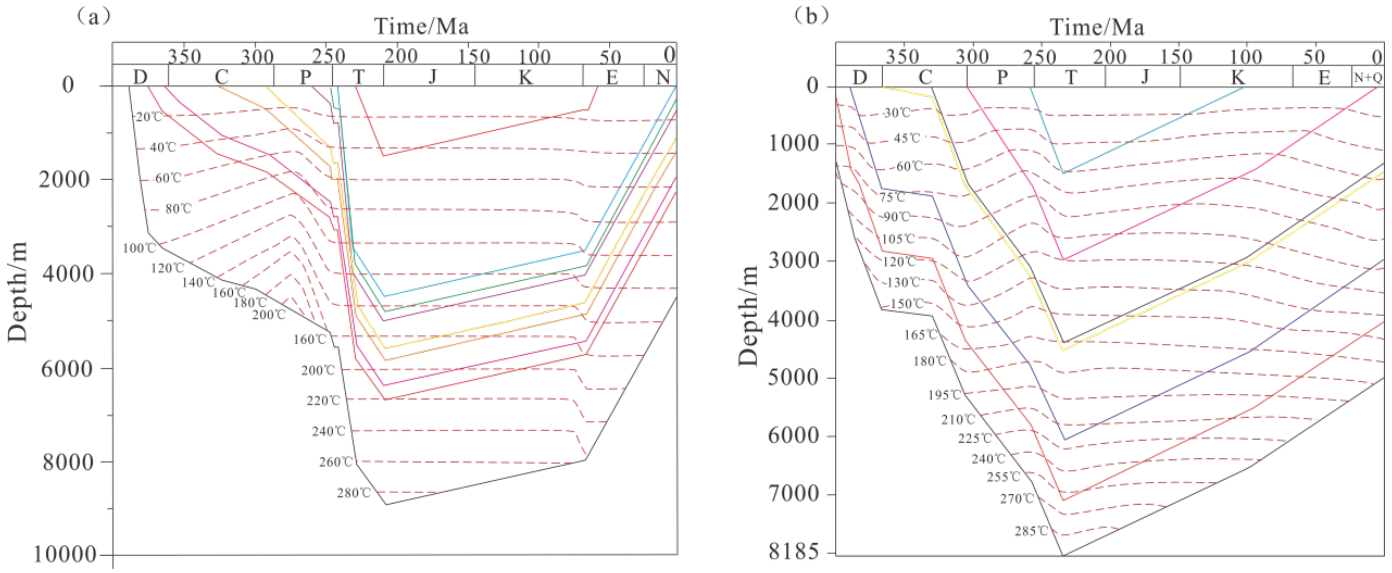

Figure 12. Burial history maps of the Nanpanjiang and northern margin of the Guizhong Depression. (a) Burial and thermal history map of the Sanglang area, eastern Nanpanjiang [38]; (b) Burial and thermal history map of Well Guizhong-1, Guizhong Depression [39].

with a breakthrough pressure of 21.0 MPa, providing an effective seal for shale gas. The tight lenticular limestone of the Wuzhishan Formation has a porosity of 1.39% and permeability approaching 0 mD, with a breakthrough pressure of 22.5 MPa. This formation serves both as a high-quality floor for the Luzhai Formation shale in the Carboniferous System and as an excellent caprock for the Huogong Formation in the Middle Devonian System.

5 Evaluation of Shale Gas Preservation Conditions

Based on a systematic analysis of shale preservation conditions, key controlling parameters—including sealing conditions, tectonic movements, and burial depth—were identified. Drawing on the extensive exploration and development experience of marine shale gas in the Sichuan Basin, a preservation evaluation index for residual syncline shale gas was established, comprising three categories and twelve parameters (Table 5).

Focusing on tectonic factors as the core, and integrating analyses of regional burial and thermal histories (Figure 12), this zoning study applied weighted coefficients to perform overlay processing of various evaluation parameters. The average clustering analysis method was then employed to classify the study area. Ultimately, a comprehensive evaluation of residual shale gas preservation conditions was achieved, resulting in the compilation of comprehensive evaluation maps for shale gas preservation in the Lower Carboniferous of the Langdai area within the Nanpanjiang Basin, as well as the Lower Carboniferous and Middle Devonian in the northern margin of the Guizhong Sag (Figures 13, 14, and 15).

Based on the research of Zhao et al. [38] on the hydrocarbon accumulation process in the Sanglang area of the eastern Nanpanjiang Basin (Figure 12(a)), it is inferred that the Lower Carboniferous shale in the Langdai area entered the gas-generating stage during the Triassic period (Ro > 1.3%). Subsequently, during the Late Indosinian period, the presence of active large-scale normal faults, strike-slip faults, and burial depth conditions were the primary factors limiting the shale gas preservation within the Langdai Syncline.

The Type I and II favorable areas for shale gas preservation in the Langdai Syncline are concentrated between the PLF-1 (Panlong Fault No. 1) and LDF-2 (Langdai Fault No. 2), within a relatively stable internal fault block zone. The burial depth increases sharply toward the southeast of the syncline. Areas adjacent to the major through-going faults with significant throws—the Yadu-Ziyun-Luodian Fault (throw of 1,365 m) and Langdai Fault (throw of 1,173 m)—are dominated by Type III favorable areas (Figure 13).

The through-going faults along the margin of the Xinzhai Syncline may compromise the shale gas preservation environment. However, a small-scale reverse fault, which does not extend to the surface, is present in the syncline core and may enhance shale

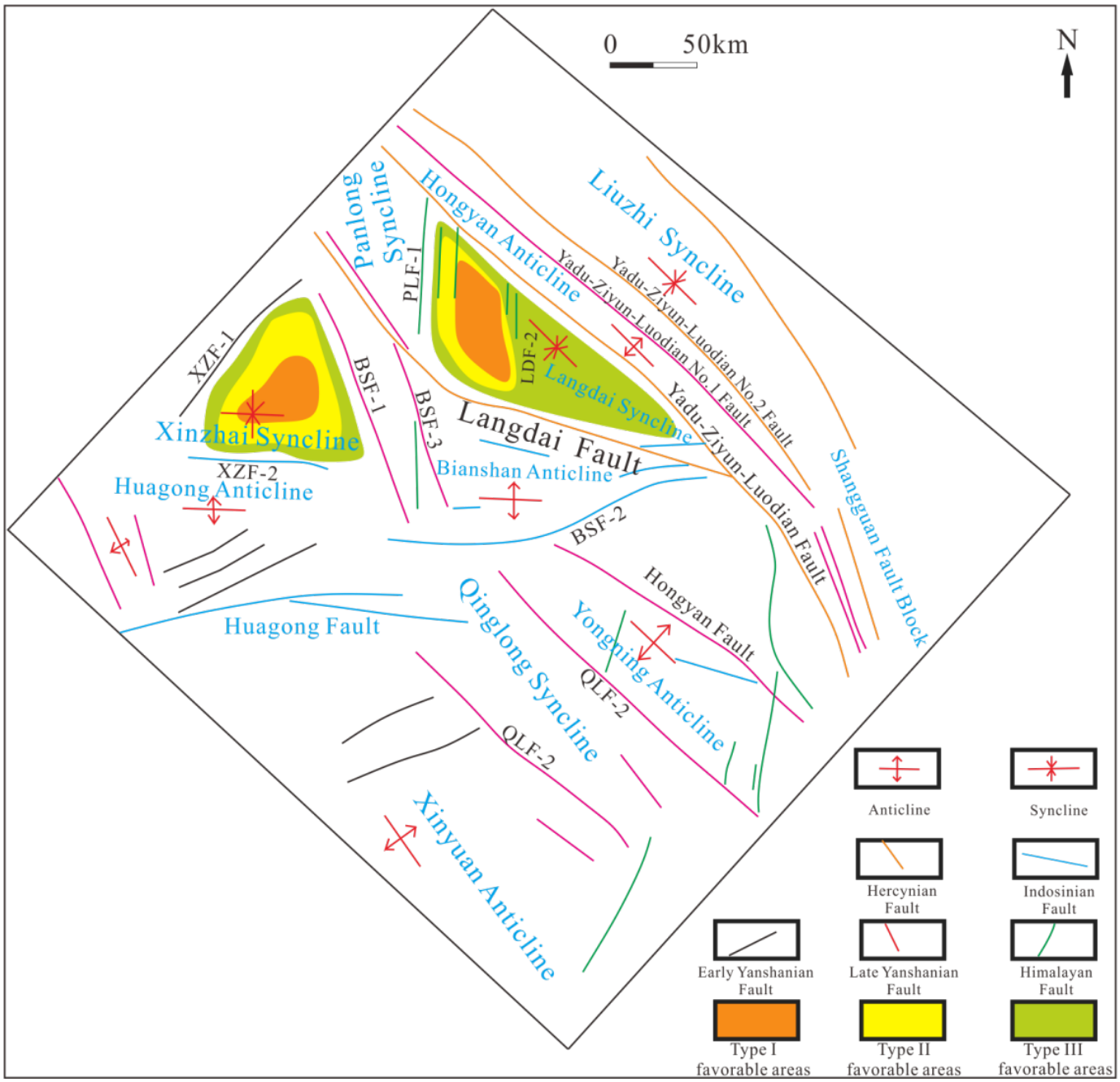

Figure 13. Comprehensive evaluation map of shale gas preservation conditions for the Lower Carboniferous in the Langdai area, Nanpanjiang Depression.

permeability. The Type I favorable area of this syncline is located in the syncline core, while the Type II and III favorable areas are distributed around the core (Figure 13).

Drawing on preservation condition analysis methodologies established for analogous marine shale systems [39], and based on burial and thermal history reconstruction of the Guizhong Depression (Figure 12(b)), it is inferred that the Lower Carboniferous shale along the northern margin of the Guizhong Depression entered the gas window during the Early Triassic (formation temperature > 120 °C), whereas the Middle Devonian shale entered the gas window during the Early Permian.

Large-scale destructive faults active during the Indosinian period and subsequent eras may have compromised the preservation conditions of the Lower Carboniferous shale. Similarly, faults active during the Hercynian period and thereafter likely impaired the preservation of the Middle Devonian shale. Additionally, the burial depth of the strata and their proximity to large-scale faults are critical

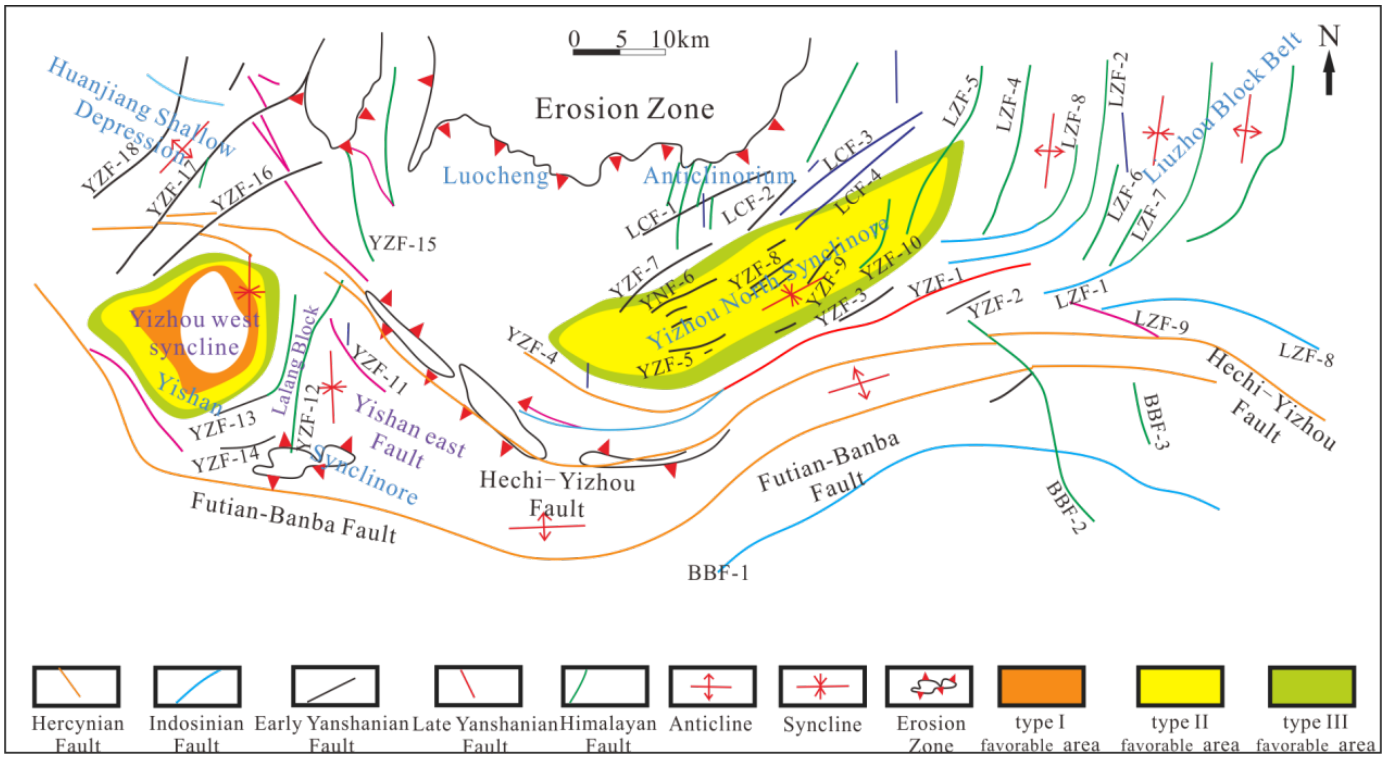

Figure 14. Comprehensive evaluation map of shale gas preservation conditions for the Lower Carboniferous in the northern margin of the Guizhong Depression.

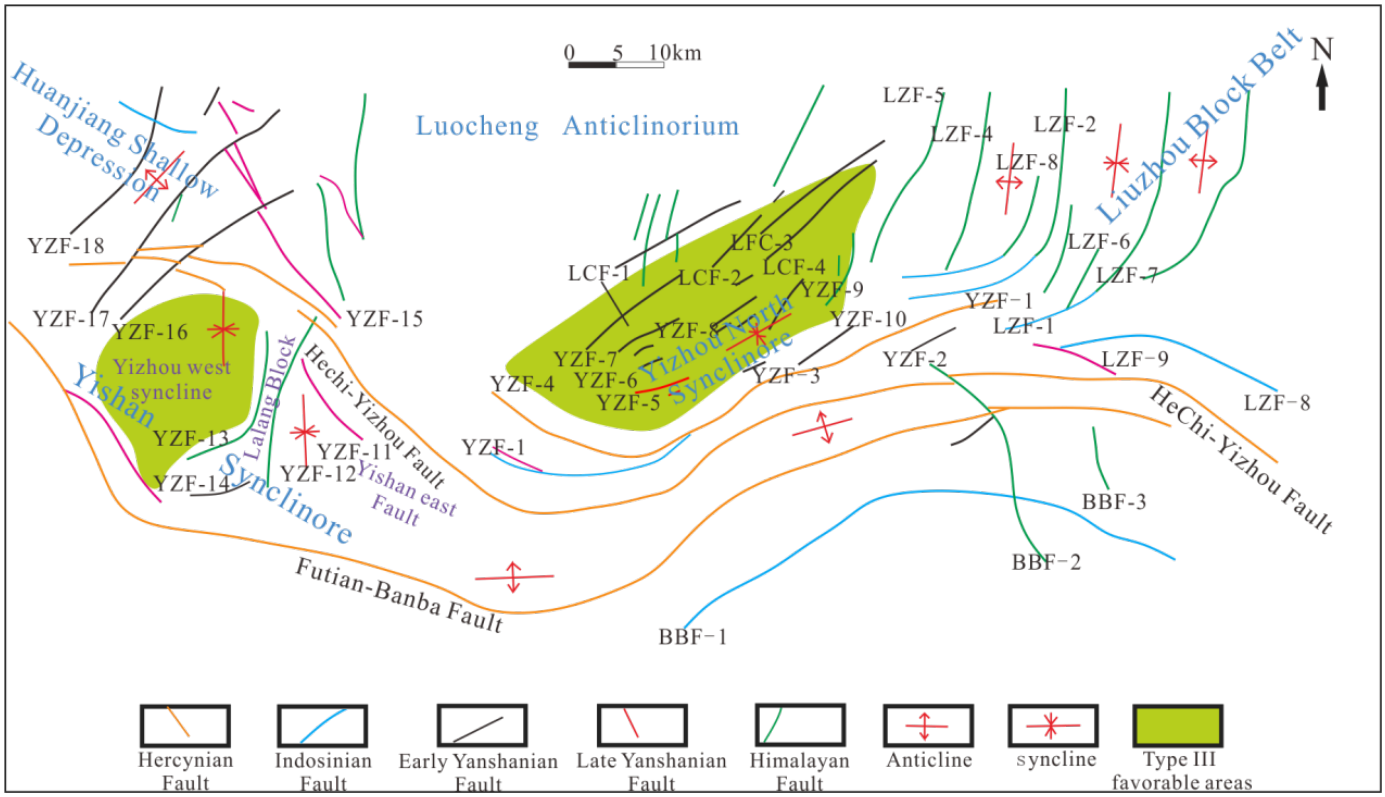

Figure 15. Comprehensive evaluation map of shale gas preservation conditions for the Middle Devonian in the northern margin of the Guizhong Depression.

factors influencing the preservation of both the Lower Carboniferous and Middle Devonian shales along the northern margin of the Guizhong Depression.

The Carboniferous strata in the North Yizhou Syncline experienced denudation in the northern region, causing the basal section to outcrop directly at the

surface. Consequently, the preservation conditions are considered relatively poor, with only Type II and III favorable areas for shale gas preservation identified (Figure 14). Similarly, the Middle Devonian strata in this syncline were also denuded toward the north and lack high-quality shale, leading to an overall classification as Type III favorable areas (Figure 15).

The basal boundary of the Carboniferous System in the West Yizhou Syncline exhibits a gentle structural configuration. Its preservation conditions are primarily influenced by the Devonian isolated platform area, as well as strike-slip and normal faults within the surrounding Lalong Fault Block. A comprehensive evaluation indicates that Type I, II, and III favorable areas are predominantly developed around the periphery of the Upper Devonian isolated platform area (Figure 14). The basal boundary of the Upper Devonian in this syncline is affected by strike-slip and normal faults in the Lalong Fault Block and lacks high-quality shale, resulting in its overall classification as a Type III favorable area (Figure 15).

6 Conclusions

(1) The Xinzhai and West Yizhou synclines exemplify gentle bidirectional thrust structures characterized by broad, gentle morphology, minimal fault development, and excellent stratigraphic continuity, thereby presenting optimal conditions for shale gas preservation. The Langdai Syncline constitutes a gentle unidirectional thrust structure, whose preservation conditions are moderately favorable despite unidirectional thrusting effects. The North Yizhou Syncline represents a gentle nappe-type thrust monocline; subjected to intense late-stage thrust nappe activity and denudation, it exhibits pronounced fault fragmentation and consequently unfavorable shale gas preservation conditions.

(2) The Yanshanian Period constitutes the principal phase of tectonic shortening for the Langdai, Xinzhai, and West Yizhou synclines, whereas the Indosinian Period represents the primary deformation phase for the North Yizhou Syncline. The Langdai (13.24%) and Xinzhai (12.49%) synclines exhibit relatively low tectonic shortening rates, which favor shale gas preservation; the West Yizhou (24.71%) and North Yizhou (41.98%) synclines display elevated tectonic shortening rates, which are detrimental to shale gas preservation. The denudation in the Langdai area is significantly weaker than that in the Guizhong area.

(3) Compressional reverse faults predominate throughout the study area, exhibiting excellent lateral sealing capacity that promotes shale gas retention. Caprock breakthrough pressures in the Langdai area (23.5–61.6 MPa) substantially exceed those in the Guizhong area (0.9–22.5 MPa), conferring superior microscale sealing capacity and enhanced vertical confinement for shale gas.

(4) Quantitative evaluation reveals that Type I favorable areas for Lower Carboniferous shale in the Xinzhai Syncline are concentrated within the synclinal core, with Type II and III favorable areas distributed annularly around the core. Type I and II favorable areas for Lower Carboniferous shale in the Langdai Syncline are situated between the PLF-1 and LDF-2, whereas the southeastern portion of the syncline is predominantly characterized by Type III favorable areas. Type I, II, and III favorable areas at the basal Carboniferous boundary in the West Yizhou Syncline are distributed peripherally around the Upper Devonian isolated platform area. Only Type II and III favorable areas are developed within the Carboniferous of the North Yizhou Syncline. The Middle Devonian strata in both the West Yizhou and North Yizhou synclines are uniformly classified as Type III favorable areas for shale gas.

Data Availability Statement

Data will be made available on request.

Funding

This work was supported by the National Natural Science Foundation of China under Grant 42272171.

Conflicts of Interest

The authors declare no conflicts of interest.

AI Use Statement

The authors declare that no generative AI was used in the preparation of this manuscript.

Ethical Approval and Consent to Participate

Not applicable.

References

[1] Zou, C., Zhao, Q., Dong, D., Yang, Z., Qiu, Z., Liang, F., Wang, N., Huang, Y., Duan, A., Zhang, Q., & Hu, Z. (2018). Geological characteristics, main challenges and future prospect of shale gas. *Natural Gas Geoscience*, *28*(12), 1781-1796. [CrossRef]

[2] Xu, Z., Hu, X., Wang, J., Ju, X., Xin, Y., Ma, C., ... & Wang, W. (2026). Shale characteristics and shale-gas potentials in the Lower Devonian Tangding Formation in the Tian'e area of the Nanpanjiang Basin, SW China. *Petroleum Geoscience, 32*(1), petgeo2024-110. [CrossRef]

[3] Qin, Y., Lei, Y., Jiang, S., Zhang, R., Zhang, L., Cen, W., & Lu, B. (2022). Shale gas accumulation conditions and resource potential evaluation of member 1 of the Lower Carboniferous Luzhai Formation in the northern Guizhong depression. *Petroleum Science Bulletin, 7*(2), 139-154. [CrossRef]

[4] Yao, H., Zhang, P., He, X., Gao, Y., Gao, Q.,Wan,J., & Zhou, D. (2025). Classification and exploration practices of shale gas reservoirs in the Wufeng-Longmaxi formations in the Sichuan Basin and its periphery. *Oil & Gas Geology, 46*(6), 1807-1822. [CrossRef]

[5] Bian, R., Sun, C., Nie, H., Liu, Z., Du, W., Li, P., & Wang, R. (2023). Types, characteristics, and exploration targets of deep shale gas reservoirs in the Wufeng-Longmaxi formations, southeastern Sichuan Basin. *Oil & Gas Geology, 44*(6), 1515-1529. [CrossRef]

[6] Yuan, K., Fang, X., Wen, T., Lin, T., Shi, D., Bao, S., ... & Zhang, C. (2017). Accumulation conditions of Devonian shale gas in well GY 1 in northwestern Central Guangxi Depression. *China Petroleum Exploration, 22*(4), 90-97. [CrossRef]

[7] Wang, Y. F., Zhai, G. Y., Shi, W. Z., Wang, J. Z., Zhang, J. Z., Kang, H. X., ... & Zhou, S. T. (2025). Factors controlling enrichment and accumulation of Devonian–Carboniferous shale gas in the Yaziluo rift trough in the Yunnan–Guizhou–Guangxi region. *Journal of Geomechanics, 31*(2), 248-266. [CrossRef]

[8] Hu, L., Xue, X., Du, W., Cheng, P., & Zi, J. (2022). Reservoir Characteristics of the Qiongzhusi Shales and Their Influencing Factors in the Qujing Area, Yunan Province. *Geological Journal of China Universities, 28*(4), 617 [CrossRef]

[9] Jiang, Z.,Song , Y., Tang, X., Li, Z., Wang, X., Wang, G., ... & Qiu, H. (2020). Controlling factors of marine shale gas differential enrichment in southern China. *Petroleum Exploration and Development, 47*(3), 661-673 [CrossRef]

[10] Zhou, W., Jiang, Z., Qiu, H., Jin, X., Wang, R., Cen, W., ... & Sun, Y. (2019). Shale gas accumulation conditions and prediction of favorable areas for the Lower Carboniferous Luzhai Formation in Guizhong depression. *Acta Petrolei Sinica, 40*(7), 798. [CrossRef]

[11] Duan, L., Meng, Q. R., Wu, G. L., Yang, Z., Wang, J., & Zhan, R. (2020). Nanpanjiang basin: A window on the tectonic development of south China during Triassic assembly of the southeastern and eastern Asia. *Gondwana Research, 78*, 189-209. [CrossRef]

[12] Jiang,H.,Wang,H.,Xiao,J.,Lin,Z.,Lv,X.,&Cai, J.(2008). Tectonic inversion and its relationship with hydrocarbon accumulation in Zhu-3 Depression of Pearl River MouthBasin. *ActaPetroleiSinica, 29*(3), 372. [CrossRef]

[13] Faure, M., Lin, W., Chu, Y., & Lepvrier, C. (2016). Triassic tectonics of the southern margin of the South China Block. *Comptes Rendus Geoscience, 348*(1), 5-14. [CrossRef]

[14] Liang, Y., Liu, Z., Chen, Y., & Liu, S. (2020). Analysis of Sequence and Sedimentary Facies in Simen Formation of Lower Carboniferous in the North-central Guizhong Depression. *Northwestern Geology, 53*(2), 27-41. [CrossRef]

[15] Liu, Y., Hu, K., Han, S., & Sun, Z. (2015). Structural evolution of the Youjiang Basin and its controlling effects on the formation of Carlin-type gold deposits. *Geological Journal of China Universities, 21*(1), 1. [CrossRef]

[16] Gu, Z., He, Y., Peng, Y., Rao, S., Du, W., & Zhang, C. (2017). Shale gas accumulation conditions of the Lower Cambrian insouthern Sichuan-central Guizhou, China. *Natural Gas Geoscience, 28*(4), 642-653. [CrossRef]

[17] Yang, W. X., Yan, D. P., Qiu, L., Wells, M. L., Dong, J. M., Gao, T., ... & Wang, F. (2021). Formation and forward propagation of the Indosinian foreland fold-thrust belt and Nanpanjiang foreland basin in SW China. *Tectonics, 40*(4), e2020TC006552. [CrossRef]

[18] Wang, J., Jiang, L., Cang, T., Zhou, X., & Wang, B. (2025). Simulation of a Multi-Stage Stress Field and Regional Prediction of Structural Fractures in the Tucheng Syncline, Western Guizhou, China. *Geosciences, 15*(4), 132. [CrossRef]

[19] Wang, Y., Du, W., Wang, Y., Lin, R., Zhang, D., Zhao, F., ... & Wang, Y. (2022). Meso-cenozoic tectonic evolution of the ziyun-luodian fault in SW China. *Frontiers in Earth Science, 10*, 970944. [CrossRef]

[20] Yuan, K., Huang, W. H., Wang, T., Li, S. Z., Sun, X. C., Fang, X. X., ... & Guo, J. (2023). Tectonic evolution and accumulation characteristics of Carboniferous shale gas in Yadu-Ziyun-Luodian aulacogen, Guizhou Province, South China. *China Geology, 6*(4), 646-659. [CrossRef]

[21] Zhao, L., He, Y., Yang, P., Chen, H., & An, Y. (2015). Characteristics of Lower Palaeozoic hydrocarbon source strata and a primary study of the shale gas accumulation in northern Guizhou Province. *Geology in China, 42*(6), 1931-1943. [CrossRef]

[22] Cui, X., Wang, G. H., Zhang, S. T., Quaye, J. A., Zhou, J., Zhang, Y. J., ... & Gao, X. (2024). Paleo-stress reconstruction and implications for the Mesozoic tectonic evolution of the Guizhong Depression, South China Block. *Geological Journal, 59*(5), 1642-1662. [CrossRef]

[23] Rouby, D., Cobbold, P. R., Szatmari, P., Demercian, S., Coelho, D., & Rici, J. A. (1993). Least-squares palinspastic restoration of regions of normal

faulting—application to the Campos basin (Brazil). *Tectonophysics, 221*(3-4), 439-452. [CrossRef]

[24] Hu, J. X., Xiao, C. H., Wei, C. S., Shen, Y. K., Chen, Z. L., Zhang, Y., & Zhang, D. (2023). Polyphase deformation of the Youjiang fold-and-thrust belt during the Mesozoic: Implications for the tectonic transition of the South China block. *Frontiers in Earth Science, 10*, 1033541. [CrossRef]

[25] Wu, J., Yan, D., Qiu, L., Pan, M., Lin, Y., Liao, J., & Wu, L. (2026). How was intraplate deformation in the Youjiang tectonic belt of southwestern South China influenced by marginal orogenesis?. *Geological Society of America Bulletin, 138*(5-6), 2023-2048. [CrossRef]

[26] Li, Y., Xue, X., Zhang, J., Li, J., Hu, L., Wang, L., & Chen, Z. (2025). Geological characteristics and gas-bearing control factors of shale gas in the Wufeng-Longmaxi Formation of the Shaozhai syncline in northeastern Yunnan. *Coal Science and Technology, 53*(5), 255-264. [CrossRef]

[27] Mu, D., Li, S., Wang, Q., Somerville, I., Wang, Y., Zhao, S., ... & Suo, Y. (2018). Early Paleozoic orocline in the Central China orogen. *Gondwana Research, 63*, 85-104. [CrossRef]

[28] Zhou, Y., Luo, L., Zeng, L., Liu, C., Liu, S., You, Y., & Mo, J. (2024). Deformation characteristics and shale gas accumulation model of the Baima structural belt in the Fuling shale gas field. *Petroleum Science Bulletin, 9*(2), 183-195. [CrossRef]

[29] Hu, D., Wei, Z., Liu, R., Fan, Z., & Han, J. (2019). Development characteristics and exploration potential of the lower carboniferous black shale in the Guizhong depression. *Natural Gas Industry B, 6*(3), 205-214. [CrossRef]

[30] Dong, Z., She, X., Xu, H., & Li, D. (2018). Thrust nappe tectonic characteristics and evolution during Indosinian-Yanshanian period in Dagang Wangguantun-Wumaying region. *Progress in Geophysics, 33*(5), 1773-1782. [CrossRef]

[31] Zhao, W., Jing, T., Wu, B., Zhou, Y., & Xiong, X. (2018). Controlling mechanism of faults on the preservation conditions of shale gas: A case study of Wufeng-Longmaxi Formations in Southeast Chongqing. *Natural Gas Geoscience, 29*(9), 11. [CrossRef]

[32] Liu, Y., Jin, J., Pan, R., Li, X., & Zhu, Z. (2023). Preservation condition evaluation of normal pressure shale gas in the Wufeng and Longmaxi Formations of basin margin transition zone, Southeast Chongqing. *Bulletin of Geological Science and Technology, 42*(1), 253-263. [CrossRef]

[33] Yu, G., Wei, X., Li, F., & Liu, Z. (2020). Disruptive effects of faulting on shale gas preservation in Upper Yangtze region. *Petroleum Geology & Experiment, 42*(3), 355-362. [CrossRef]

[34] Feng, Q., Qiu, N., Borjigin, T., Wu, H., Zhang, J., Shen, B., & Wang, J. (2022). Tectonic evolution revealed by thermo-kinematic and its effect on shale gas preservation. *Energy, 240*, 122781. [CrossRef]

[35] Bai, D., Xiong, X., Yang, J., Zhong, X., Ha, P., & Uhang, W. (2014). Geological structure characteristics of the middle segment of the Xuefeng orogen. *Geology in China, 41*(2), 399-418. [CrossRef]

[36] Zhang, K., Ma, D., Xiangli, H., & Shao, K. (2016). New Progress on the Research of Formation Mechanism of Shale Gas Reservoir. *Clean Coal and Energy, 4*(2), 9-15. [CrossRef]

[37] Liang, F., Zhu, Y., Qi, L., Wang, H., Bai, W., Ma, C., Zhang, Q., & Cui, H. (2016). Accumulation condition and gas content influence factors of Niutitang Formation organic-rich shale in Changde area, Hunan Province. *Natural Gas Geoscience, 27*(1), 180-188. [CrossRef]

[38] Zhao, M., Zhang, S., Zhao, L., & Da, J. (2007). Geochemical features and genesis of the natural gas and bitumen in paleo-oil reservoirs of Nanpanjiang Basin, China. *Science in China Series D: Earth Sciences, 50*(5), 689-701. [CrossRef]

[39] Jiang, S., Zhou, Q., Li, Y., & Yang, R. (2024). A case study on preservation conditions and influencing factors of shale gas in the Lower Paleozoic Niutitang Formation, western Hubei and Hunan, middle Yangtze region, China. *Geofluids, 2024*(1), 6637899. [CrossRef]

Lingying Huang received the B.Eng. degree from Southwest Petroleum University, Chengdu, Sichuan, China, in 2024. (Email: 202421000117@stu.swpu.edu.cn)

Yifan Gu received the Ph.D. degree from Southwest Petroleum University, Chengdu, Sichuan, China, in 2020. (Email: xnsygyf@126.com)

Yuqiang Jiang received the M.Eng. degree from Southwest Petroleum University, Chengdu, Sichuan, China, in 1993. (Email: xnsyjyq3055@126.com)